

Electroweak Physics in Six-Fermion Processes at Future Colliders*

F. Piccinini^a

^aIstituto Nazionale di Fisica Nucleare, Sezione di Pavia,
Dipartimento di Fisica Nucleare e Teorica, Università di Pavia,
Pavia, Italy

Recent developments in the field of complete electroweak tree-level calculations for six-fermion final states in e^+e^- collisions are briefly reviewed. Particular attention is given to *top*-quark and Higgs boson physics, which are items of primary importance at the Next Linear Collider. The relevance of electroweak backgrounds and finite-width effects is discussed, showing the importance of complete calculations for precision studies at the colliders operating in the TeV energy range.

1. Introduction

Many signals of interest for tests of the Standard Model and search for new physics at the Next Linear Collider (NLC) will be given by many-particle final states. In particular, the six-fermion signatures will be relevant to several subjects, such as *top*-quark physics, intermediate-mass Higgs boson production and the analysis of anomalous gauge couplings. Each of these topics can be considered as a signal by itself or as a background for another one. Assuming a realistic luminosity of $500 \text{ fb}^{-1}/\text{yr}$, the statistical errors on several six-fermion signatures are at the per cent level, so that “precision” calculations that take into account all background, finite width and final-state correlation effects are needed. In this contribution some theoretical issues concerning six-fermion channels relevant for *top*-quark and Higgs boson physics are addressed. A first study of the impact of quartic anomalous gauge couplings has been performed in ref. [1]. For the sake of brevity, this subject will not be reviewed in the present contribution.

The numerical results presented have been performed by means of the computer code SIXFAP [2], that involves the algorithm ALPHA [3],

for the automatic calculation of the scattering amplitudes, and a Monte Carlo integration procedure derived from the four-fermion codes HIGGSPV [4] and WGENPV [5], and developed to deal with six-fermion processes. The code has been adapted to deal with a large variety of diagram topologies, including both charged and neutral currents, so as to keep under control all the relevant signals of interest as well as the complicated backgrounds that are involved in six-fermion processes where hundreds of diagrams contribute to the tree-level amplitudes. The effects of initial state radiation (ISR) and beamsstrahlung (BS) are also included.

2. *Top*-quark physics in six-quark processes

The production of a $t\bar{t}$ pair gives rise to six fermions in the final state. The $6f$ signatures relevant to the study of the *top* quark in e^+e^- collisions can be summarized as follows: $b\bar{b}l\nu_l l'\nu_{l'}$ (leptonic, $\sim 10\%$ of the total rate), $b\bar{b}q\bar{q}'l\nu_l$ (semi leptonic, $\sim 45\%$), $b\bar{b} + 4q$ (hadronic, $\sim 45\%$). Semi leptonic signatures have been considered in refs. [6–8]. It is then of great interest to carefully evaluate the size of the totally hadronic, six-quark ($6q$) contributions to integrated cross-sections and distributions as well as to determine their phenomenological features [9,10].

The $6q$ signatures of the form $b\bar{b} + 4q$, with $q = u, d, c, s$, are considered and the results of

*Presented at *Loops and Legs in Quantum Field Theory*, April 2000, Bastei, Germany. Based on work done in collaboration with F. Gangemi, G. Montagna, M. Moretti and O. Nicrosini.

complete electroweak tree-level calculations are presented. In particular the rôle of electroweak backgrounds and of ISR and BS are studied. The QCD contributions, which however play a significant rôle, are not considered.

In Tab. 1 all the electroweak processes contributing to the signature of six quarks in the final state with one $b\bar{b}$ pair are listed. While the CC processes receive contribution from the $t\bar{t}$ production Feynman diagrams only, to the MIXED processes contribute both signal and background as well as their interferences diagrams. The purely NC processes do not contribute to the signal.

CC only	MIXED	NC only
$bbud\bar{c}s$	$bbud\bar{u}d$	$bbu\bar{u}s\bar{s},$ $b\bar{b}c\bar{c}d\bar{d}$
$b\bar{b}udc\bar{s}$	$b\bar{b}c\bar{s}c\bar{s}$	$b\bar{b}u\bar{u}u\bar{u},$ $b\bar{b}c\bar{c}c\bar{c}$ $b\bar{b}d\bar{d}d\bar{d},$ $b\bar{b}s\bar{s}s\bar{s}$ $b\bar{b}u\bar{u}c\bar{c}$ $b\bar{b}d\bar{d}s\bar{s}$

Table 1

Six-quark final states with only one $b\bar{b}$ pair. The notations CC (charged currents) and NC (neutral currents) refer to the currents formed by the quark flavours different from b .

The integrated cross-section for $e^+e^- \rightarrow 6q$ with one $b\bar{b}$ pair is shown in fig. 1 in the energy range between 350 and 800 GeV for $m_h = 185$ GeV and for a realistic set of cuts specified in the figure. The effect of the electroweak backgrounds is pointed out by comparing the solid line, obtained with the full six-fermion calculation, with the dotted one, which corresponds to the contribution of the signal Feynman diagrams only. As can be seen, the contribution of the electroweak backgrounds reach the size of 10% over all the center of mass (c.m.) energy spectrum. The results of a calculation taking into account the effect of ISR on the signal only are shown with the dashed-dotted line. The effects of ISR

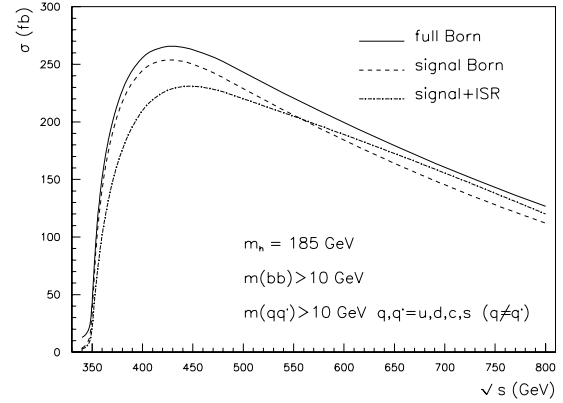


Figure 1. Full six-quark electroweak cross section (solid line) and $t\bar{t}$ signal (dashed line) in the Born approximation, and $t\bar{t}$ signal with ISR (dash-dotted line), as a function of the c.m. energy.

can be of the order of 30% near threshold, where the Born cross-section has a steep increasing, and reduce to higher energies.

A complete six-fermion calculation can also be used to study the reliability of the cross-section calculation performed in the narrow width approximation (NWA), where the top -quark is treated as a real particle, with the advantage of handling a simple calculation. As shown in ref. [9] this approximation is valid at very high energy, but it overestimates the cross-section of about 10% near the threshold.

The total electroweak cross-section has also been studied at the threshold for $t\bar{t}$ production as a function of the Higgs boson mass. Although the dominant effects in this case come from QCD contributions, as is well known [11], the electroweak backgrounds turn out to give a sizeable uncertainty, of the order of 10% of the pure electroweak contribution, in the intermediate range of Higgs boson masses (see fig. 2), which is related to the

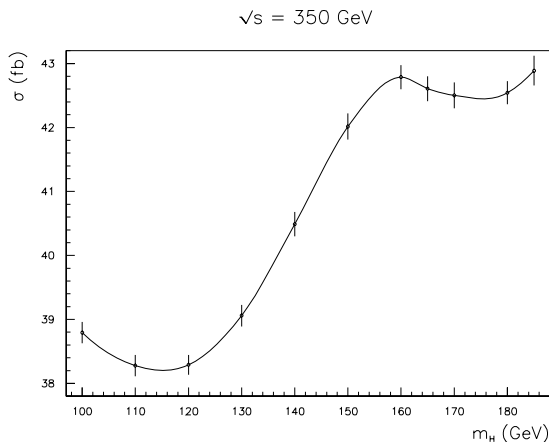


Figure 2. Total cross-section as a function of the Higgs boson mass at the threshold for $t\bar{t}$ production.

fact that the Higgs boson mass is not known. Furthermore, even if the Higgs boson mass value will be known at the run time of the NLC, its experimental error will translate into a theoretical uncertainty on the threshold cross-section determination, especially if the central value lies in the interval 120-160 GeV.

In order to study the possibility of isolating the top -quark signal from the QCD backgrounds, the topology of the events can be studied by means of the event-shape variables. The pure QCD contributions have been analysed in ref. [12]. In fig. 3 the thrust distribution of the electroweak contribution is shown at a c.m. energy of 500 GeV and with a Higgs boson mass of 185 GeV in the Born approximation (dashed histogram) and with ISR and BS (solid histogram). The invariant masses of the $b\bar{b}$ pair and of all the pairs of quarks other than b are required to be greater than 10 GeV. Remarkable effects due to ISR and BS can be seen in this plot, where the peak in the thrust distribution is strongly reduced with respect to the Born approximation and the events are shifted towards

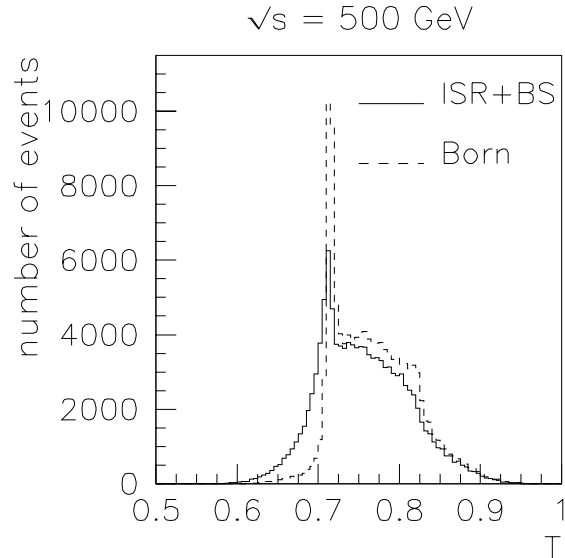


Figure 3. Thrust distribution in the Born approximation (dashed histogram) and with ISR and BS (solid histogram), at a c.m. energy of 500 GeV and for a Higgs boson mass of 185 GeV. The invariant masses of the $b\bar{b}$ pair and of all the pairs of quarks other than b are required to be greater than 10 GeV.

the lower values of T , which correspond to spherical events. In view of the results of ref. [12], the thrust variable is very effective in discriminating pure QCD backgrounds, also in the presence of electroweak backgrounds and of ISR and BS. Going up with the c.m. energy, the peak in the thrust distribution approaches the maximum allowed value, so it becomes more difficult at energies of the order of 1 TeV to discriminate between electroweak contributions and QCD backgrounds [9].

3. Intermediate-mass Higgs boson

The current lower bound on the Higgs boson mass deduced from direct search at LEP is 108 GeV at 95 % C.L. [13], while the upper bound given by fits to the precision data on electroweak observables is 188 GeV at 95 % C.L. (280 GeV at

95 % C.L. in a Bayesian approach) [13].

In the mass range favoured by the present experimental information, the relevant signatures at the NLC are four-fermion final states if the Higgs boson mass is below 130-140 GeV, and six-fermion final states if the Higgs boson mass is greater than 140 GeV. The processes of the first kind have been extensively studied in connection with physics at LEP, while those of the second kind have only recently been addressed [6,10,14,15].

In this section some aspects of complete electroweak tree-level calculations for the processes $e^+e^- \rightarrow q\bar{q}l^+\nu\bar{\nu}$, with $q = u, d, c, s$, $l = e, \mu, \tau$ and $\nu = \nu_e, \nu_\mu, \nu_\tau$ are presented. These processes are characterized by the presence of both charged and neutral currents and of different mechanisms of Higgs boson production involving Higgs-strahlung and vector boson fusion; moreover, QCD backgrounds are absent.

The total cross-section is shown in fig. 4 as a function of the c.m. energy for three values of the Higgs boson mass, with suitable kinematical cuts, to avoid the soft-pair singularities. The increase with energy, common to all three curves in fig. 4, is due, at high energies, to the t -channel contributions; in the case of $m_H = 255$ GeV, the steep rise near $\sqrt{s} = 360$ GeV is related to the existence of a threshold effect for the Higgs-strahlung process at an energy $\sqrt{s} \sim m_H + M_Z$. Thanks to the sums over quark, charged lepton and neutrino flavours, as well as the combined action of different production mechanisms, assuming a luminosity of $500 \text{ fb}^{-1}/\text{yr}$ and a Higgs mass of, say, 185 GeV, more than 1000 events can be expected at a c.m. energy of 360 GeV and more than 2000 at 800 GeV.

In the framework of a six-fermion calculation, the only meaningful procedure for a cross section evaluation is based on the sum of all the tree-level Feynman diagrams. On the other hand, there is a number of reasons to consider a subset of diagrams that can be defined as the Higgs boson signal and to define a corresponding background. First of all, this is of great interest from the point of view of the search for the Higgs boson in the experiments. Moreover, such a definition allows one to make a comparison with results obtained

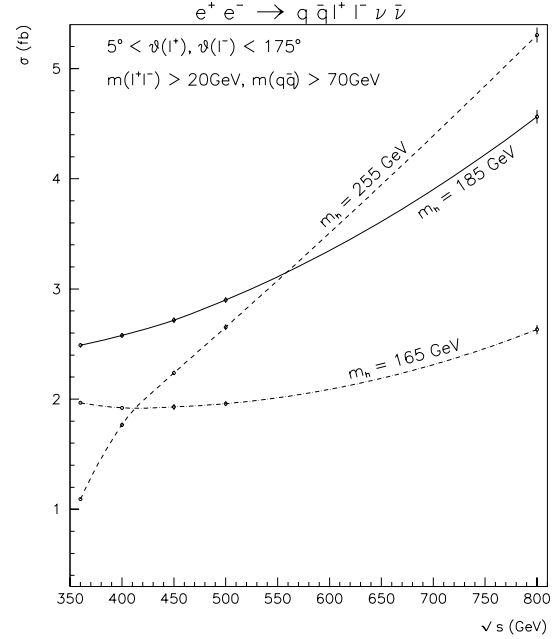


Figure 4. Total cross section for the process $e^+e^- \rightarrow q\bar{q}l^+\nu\bar{\nu}$ in the Born approximation, as a function of \sqrt{s} for three different values of the Higgs boson mass m_H . The angles $\theta(l^+)$, $\theta(l^-)$ of the charged leptons with the beam axis are in the interval 5° - 175° , the e^+e^- and the $q\bar{q}$ invariant masses are larger than 20 GeV.

in the NWA [16]–[18], which are the only available estimations unless a complete $6f$ calculation is performed. In principle, whenever a subset of diagrams is singled out, gauge invariance may be lost and unitarity problems may arise. However, in the literature [15], an operative definition of signal and background has been considered and its reliability has been studied for various Higgs boson masses and c.m. energies.

The Higgs boson signal for a given six-fermion final state is defined as the sum of the graphs containing a resonant Higgs boson. The background is defined as the sum of all the diagrams without a Higgs boson. However, there are Feynman diagrams with a non-resonant Higgs boson exchanged with space-like momentum, which are neither accounted for in the signal, nor in the background. Such a choice has been dictated

by the fact that these non-resonant contributions cannot correctly be included in the signal, since they cannot find a counterpart in the NWA, and because of gauge cancellations with background contributions at high energies; however, as they depend on the Higgs boson mass, they should not be included in the background as well. In order to give a quantitative estimate of the validity of this definition, the total cross section (sum of all the tree-level $6f$ Feynman diagrams) is compared in ref. [15] with the incoherent sum of signal and background. A result of this study is that up to 500 GeV the total cross section and the incoherent sum of signal and background are indistinguishable at a level of accuracy of 1%, and the definition of signal may be considered meaningful; at higher energies, the separation of signal and background starts to be less reliable, since it requires to neglect effects that are relevant at this accuracy. In particular, at 800 GeV the deviation is of the order of a few per cent and it decreases when the Higgs boson mass passes from 165 to 185 and to 255 GeV. The results are also slightly dependent on the applied cuts on the final state particles.

After having tested the reliability of the Higgs boson signal definition in a complete tree-level calculation, it is very interesting to study the accuracy of a theoretical prediction obtained within the NWA, which is much easier to perform than a full six-fermion calculation. A comparison with the NWA is shown in fig. 5 for the processes $e^+e^- \rightarrow q\bar{q}e^+e^-\nu\bar{\nu}$ and $e^+e^- \rightarrow q\bar{q}\mu^+\mu^-\nu\bar{\nu}$, where no kinematical cuts are applied and the results are in the Born approximation. Here σ_{sig} is the signal cross section, containing the contributions of the signal diagrams and their interferences. The cross section in the NWA, σ_{NWA} , is obtained in the following way (for definiteness the case with e^+e^- in the final state is considered): the known cross sections for the processes of real Higgs boson production $e^+e^- \rightarrow h\nu\bar{\nu}, he^+e^-$ [17,18] and $e^+e^- \rightarrow Zh$ [16] are multiplied by the appropriate branching ratios; then the incoherent sum of these terms is taken. Thus the comparison between σ_{sig} and σ_{NWA} gives a measure of interference between the different production mechanisms and of off-shellness effects together.

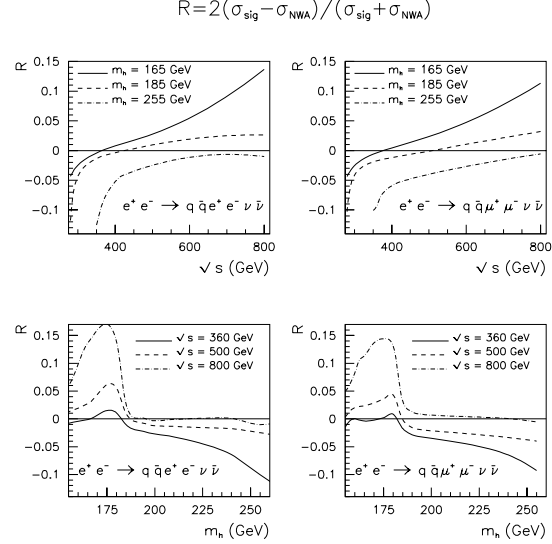


Figure 5. Comparison between the signal cross section obtained by a diagrammatic six-fermion calculation and the one calculated in the NWA (see the discussion in the text), as a function of \sqrt{s} (upper row) and of the Higgs boson mass (lower row).

As can be seen in fig. 5, the relative difference R is of the order of some per cent, depending on the Higgs boson mass and the c.m. energy; in some cases it reaches values of more than 10%, with no substantial difference between the two final states considered.

The size of the off-shellness effects, comparable with the ISR lowering, indicates the importance of a full $6f$ calculation in order to obtain sensible phenomenological predictions.

4. Conclusions

The six-fermion final states will be among the most relevant new signatures at future e^+e^- Linear Colliders. In particular they are interesting for $t\bar{t}$ production, for Higgs boson physics in the intermediate mass range and for the study of

anomalous gauge couplings. Some aspects concerning the first two items have been reviewed in this contribution. The results presented have been obtained by means of a Monte Carlo event generator [2], developed for complete tree-level calculations of six-fermion final states at the energies of the NLC, supplemented with the effects of ISR and BS.

In this contribution the importance of complete electroweak tree-level calculations has been pointed out both for $t\bar{t}$ and for Higgs boson production in some specific channels. In particular the effects of backgrounds and finite widths have been studied and compared with the predictions obtained in the NWA, which are available in the literature. These effects turn out to be in many cases well above the per cent level, so they need to be taken into account in realistic analysis at the NLC. Moreover, the presence of a complete six-fermion final state generator allows to study all kinds of final-state distributions such as invariant masses, angular correlations and event-shape variables, that are essential both for the detection of the signals of interest and for the analysis of the properties of the particles under study.

Acknowledgements

The author wishes to thank the organizers, especially J. Blümlein and T. Riemann, for the kind invitation and the pleasant atmosphere during the workshop. The author is grateful to F. Gangemi, G. Montagna and O. Nicrosini for a careful reading of the manuscript.

REFERENCES

1. F. Gangemi, hep-ph/0002142.
2. F. Gangemi, G. Montagna, M. Moretti, O. Nicrosini and F. Piccinini, a program for realistic six-fermion signatures simulation, unpublished.
3. F. Caravaglios and M. Moretti, Phys. Lett. **B358** (1995) 332.
4. Program HIGGSPV, by G. Montagna, O. Nicrosini and F. Piccinini; write up in [19,20].
5. Program WWGENPV, by G. Montagna, O. Nicrosini and F. Piccinini; write up in [19,20]. See also G. Montagna, O. Nicrosini and F. Piccinini, Comput. Phys. Commun. **90** (1995) 141; D.G. Charlton, G. Montagna, O. Nicrosini and F. Piccinini, Comput. Phys. Commun. **99** (1997) 355.
6. E. Accomando, A. Ballestrero and M. Pizzio, Nucl. Phys. **B512** (1998) 19; in R. Settles (ed.) “ e^+e^- Linear Colliders: Physics and Detector Studies, Part E”, DESY 97-123E, p. 31; Nucl. Phys. **B547** (1999) 81; A. Ballestrero, Acta Phys. Pol. **B29** (1998) 2811.
7. F. Yuasa, Y. Kurihara and S. Kawabata, Phys. Lett. **B414** (1997) 178.
8. S. Moretti, Eur. Phys. J. **C9** (1999) 229.
9. F. Gangemi, G. Montagna, M. Moretti, O. Nicrosini and F. Piccinini, Nucl. Phys. **B559** (1999) 3.
10. F. Gangemi, G. Montagna, M. Moretti, O. Nicrosini and F. Piccinini, hep-ph/0001065, to appear in DESY 97-123F.
11. T. Teubner, Acta Phys. Polon. **B30** (1999) 1941, and refs. therein.
12. S. Moretti, Phys. Lett. **B420** (1998) 367; Nucl. Phys. **B544** (1999) 289.
13. G. Quast, these proceedings.
14. G. Montagna, M. Moretti, O. Nicrosini and F. Piccinini, Eur. Phys. J. **C2** (1998) 483.
15. F. Gangemi, G. Montagna, M. Moretti, O. Nicrosini and F. Piccinini, Eur. Phys. J. **C9** (1999) 31.
16. J. Ellis, M.K. Gaillard and D.V. Nanopoulos, Nucl. Phys. **B106** (1976) 292; J.D. Bjorken, SLAC Report 198 (1976).
17. G. Altarelli, B. Mele and F. Pitolli, Nucl. Phys. **B287** (1987) 205.
18. M. Krämer, W. Kilian and P.M. Zerwas, Phys. Lett. **B373** (1996) 135.
19. D. Bardin, R. Kleiss (conv.), “Event Generators for WW Physics”, in [21], vol. 2, p. 3.
20. M.L. Mangano, G. Ridolfi (conveners), “Event Generators for Discovery Physics”, in [21], vol. 2, p. 299.
21. G. Altarelli, T. Sjöstrand and F. Zwirner, eds., *Physics at LEP2*, CERN Report 96-01 (Geneva, 1996), vols. 1 and 2.